

Giant Spontaneous Depolarizing Potentials in the Developing Thalamic Reticular Nucleus

Susanne Pangratz-Fuehrer,¹ Uwe Rudolph,² and John R. Huguenard¹

¹Department of Neurology and Neurological Sciences, Stanford University School of Medicine, Stanford, California; and ²Laboratory of Genetic Neuropharmacology, McLean Hospital, Mailman Research Center, Harvard Medical School, Belmont, Massachusetts

Submitted 20 June 2006; accepted in final form 19 January 2007

Pangratz-Fuehrer S, Rudolph U, Huguenard JR. Giant spontaneous depolarizing potentials in the developing thalamic reticular nucleus. *J Neurophysiol* 97: 2364–2372, 2007. First published January 24, 2007; doi:10.1152/jn.00646.2006. The thalamic reticular nucleus (nRt) provides a major source of inhibition in the thalamo-cortical circuit and is critically involved in the generation of spindle oscillations. Here we describe the properties of thalamic giant depolarizing potentials (tGDPs) that were observed in nRt during early development. tGDPs persisted in presence of ionotropic glutamate antagonists but were completely abolished by GABA_AR antagonist SR 35591. tGDPs occurred primarily between p3 and p8 (in 30–50% of cells) and occasionally up until p15. tGDPs lasted 0.4–3 s with peak conductances of 2–13 nS and occurred at frequencies between 0.02 and 0.06 Hz. We used mice with a benzodiazepine-insensitive $\alpha 3$ subunit [$\alpha 3$ (H126R)] to probe for the identity of the GABA receptors responsible for tGDP generation. Benzodiazepine enhancement of tGDP amplitude and duration persisted in nRt neurons in $\alpha 3$ (H126R) mice, indicating that the GABA_ARs containing $\alpha 3$ are not critical for tGDP generation and suggesting that tGDPs are mediated by GABA_ARs containing the $\alpha 5$ subunit, which is transiently expressed in nRt neurons in early postnatal development. Furthermore we found that exogenous GABA application depolarized nRt neurons younger than p8, indicating elevated $[Cl^-]_i$ at this developmental stage. Taken together, these data suggest that in immature nRt, long-lasting depolarizing responses mediated by GABA receptors could trigger Ca^{2+} entry and play a role in functional development of the spindle-generating circuitry.

INTRODUCTION

In the adult mammalian CNS, the GABAergic nucleus reticularis thalami (nRt) is central to rhythm generating circuitry related to sleep and wakefulness within the thalamo-cortical network. Reciprocal connections between nRt and thalamo-cortical (TC) relay neurons enable intra-thalamic oscillatory activity. The synaptic release of GABA from nRt leads to inhibition of TC neurons and the triggering of rebound bursts, which in turn provide excitatory feedback to nRt, thus completing a reciprocal loop (Huguenard and Prince 1994; Steriade et al. 1985; Warren and Jones 1997). These intra-thalamic oscillations, which can occur spontaneously, are thought to be the basis for spindle rhythmicity; however, some evidence suggests that the intra-nRt circuit itself may in some cases act as pacemaker (Destexhe et al. 1994; Steriade et al. 1987). Inhibitory connectivity within nRt regulates inhibitory output and suppresses synchrony by decreasing release of GABA onto TC cells (Huguenard and Prince 1994; Huntsman

et al. 1999; Sohal et al. 2000; von Krosigk et al. 1993; Warren et al. 1994). In contrast, the uncontrolled release of GABA could lead to the pathological hypersynchrony of sleep spindles and related rhythms and may be a factor in childhood absence seizures (Steriade and Llinas 1988).

The physiological pattern of sleep spindles is absent in infants up until the second month of age (Lenard 1970; Metcalf 1970), in rodents until postnatal day 10–12 (p10–12) (Jouvet-Mounier et al. 1970) and in ferrets up until p22 (McCormick et al. 1995). This suggests that GABAergic inhibition mediated by nRt undergoes developmental maturation. Therefore we explored the properties of GABAergic synaptic inhibition in developing mouse nRt prior to the emergence of spindle oscillations. Unexpectedly, we observed the presence of thalamic giant depolarizing potentials (tGDPs) during the first 2 wk of postnatal life. This spontaneous neuronal pattern is mediated by GABA_A receptors (GABA_ARs). Similar patterns have been reported in neocortex (Yuste et al. 1992), retina (Feller 1999; Wong 1999), spinal cord (Gonzalez-Islas and Wenner 2006; Spitzer 2002), brain stem (Gummer and Mark 1994), and hippocampus (Cherubini et al. 1991; Garaschuk et al. 1998), where they appear to be Ca^{2+} dependent. The discovery of spontaneous network activity in developing systems (Ben Ari et al. 1990; Goodman and Shatz 1993; Katz and Callaway 1992; Meister et al. 1991; Wong et al. 1993; Yuste et al. 1992) raised the possibility that correlated patterns contribute to functional maturation of neonatal circuitry. In the present study, we focus on the developmental profile and pharmacological properties of tGDPs, a novel pattern of the immature intra-reticular network.

METHODS

Animals

Wild-type and mutant mice [$\alpha 3$ (H126R)] pups of either sex were used at postnatal days 3–20 (p3–p20). Mutants were mice homozygous for a histidine-to-arginine point mutation at position 126 of the GABA_A receptor $\alpha 3$ subunit (5–6 backcrosses to the 129/SvJ background) that were generated as described previously (Low et al. 2000).

Thalamic slice preparation

Experiments were performed in accordance with approved procedures (Protocol 12321/0) established by the Administrative Panel on Laboratory Animal Care at Stanford University. Mice were deeply

Address for reprint requests and other correspondence: J. R. Huguenard, Dept. of Neurology and Neurological Sciences, Stanford University School of Medicine, Stanford, CA 94305 (E-mail: John.Huguenard@stanford.edu).

The costs of publication of this article were defrayed in part by the payment of page charges. The article must therefore be hereby marked “advertisement” in accordance with 18 U.S.C. Section 1734 solely to indicate this fact.

anesthetized by intraperitoneal injection with pentobarbital (50 mg/kg) until unresponsive and then decapitated. Brains were blocked, removed and placed in ice-cold (4°C), oxygen-equilibrated (95% O₂-5% CO₂) "cutting" solution (containing in mM: 234 sucrose, 11 glucose, 24 NaHCO₃, 2.5 KCl, 1.25 NaH₂PO₄, 10 MgSO₄, and 0.5 CaCl₂) for ~1 min. Horizontal slices (200 μm) were cut with a Vibratome (TPI, St. Louis, MO), hemi-sectioned and incubated in a preheated (32°C) oxygen-equilibrated chamber filled with artificial CSF (ACSF) (containing in mM: 126 NaCl, 26 NaHCO₃, 10 glucose, 2.5 KCl, 2 MgCl₂·6H₂O, 2 CaCl₂·2H₂O, and 1.25 NaH₂PO₄·H₂O) for 1 h before recording.

Electrophysiology

Whole cell patch-clamp recordings were obtained from nRt neurons in a chamber with a constant flow of ACSF perfusion (2 ml/min) equilibrated with 95% O₂-5% CO₂. Experiments were conducted at room temperature. Glass electrodes (tip resistance: 2.5–3.3 MΩ, KG-33, borosilicate glass, Garner Glass, Claremont, CA) were pulled in multiple stages using a Flaming-Brown micropipette puller (model P-87, Sutter Instruments, Novato, CA). For voltage-clamp recordings, pipettes were filled with high (139 mM) chloride solution [containing in mM: 135 CsCl, 5 lidocaine *N*-ethyl bromide (QX-314), 2 MgCl₂, 10 ethyleneglycol-bis (β -aminoethyl ether)-*N,N,N',N'*-tetraacetate acid (EGTA; Sigma, St. Louis, MO), and 10 HEPES. The solution was adjusted with CsOH to pH 7.3]. The solution was adjusted with KOH to pH 7.3).

Voltage-clamp recordings were made from visually identified neurons within nRt using a fixed-stage upright microscope (Axioskop, Zeiss, Thornwood, NY) equipped with an insulated $\times 63$ objective, Normarski optics and an infrared-sensitive video camera (Cohu, San Diego, CA). Only one experiment per slice was performed to study pharmacology (*n* of slices), whereas up to two cells per slice were recorded to describe developmental changes (*n* of cells). Access resistance of all recorded cells was monitored constantly throughout each experiment and only used for analysis if it was <18 MΩ and stable (25% tolerance) for the duration of the experiment.

tGDP identification

The voltage-clamp manifestations of tGDPs were recorded at a holding potential of -60 mV and appeared under these recording conditions as inward currents. tGDPs were identified based on three criteria including minimum amplitude, duration, and number of individual components within each event (see RESULTS). The following properties of tGDPs (*n* > 10 events/cell) were determined: time to peak (TTP), the time required to rise from onset to peak amplitude, 90% width (the time required to decay by 90% from peak amplitude), peak current amplitude and interevent interval (IEI). To confirm that tGDPs represent distinct events and not just the occurrence of multiple concurrent spontaneously occurring inhibitory postsynaptic currents (sIPSCs), we integrated baseline-corrected voltage-clamp recordings, using a sweep length of 2 s. Histograms of net charge per 2-s period revealed two distinct populations (e.g., Fig. 3), confirming that tGDPs are not simply summated sIPSCs.

The onset of each tGDP was defined as the time of occurrence of the first component of a multiphasic response. The first component was defined as the last event before the tGDP that did not fully decay to baseline. The IEIs between tGDPs were determined for each recording. Patterns were defined as "regular" when the coefficient of variation for IEI was ≤ 0.4 , whereas "irregular" tGDP patterns were defined as having coefficients of variation >0.4.

Pharmacology and method of application

GABA_AR mediated tGDPs were recorded in the presence of (\pm)-2-amino-5-phosphopentanoic acid (APV, 100 μM, Sigma), 6,7-

dinitro-quinoxaline-2,3-dione (DNQX, 20 μM, RBI, Natick, MA) to block ionotropic glutamate receptors. Concentrated solutions of clonazepam (CZP, 100 nM) and gabazine (GBZ, 10 μM; all Sigma) were stored at -20°C, diluted with ACSF before experiments and were applied via multi-barrel local perfusion unless otherwise stated.

Data collection and analysis

Data were filtered at 2 kHz, collected, and sorted with locally written software [Metatape, WDetecta and WinScanSelect (J. R. Huguenard)], then analyzed using PClamp 9 (Axon Instruments, Union City, CA) and Origin (MicroCal Software, Inc., Northampton, MA). Data are presented as the means \pm SE. Student's *t*-test was used to assess statistical significance unless otherwise stated and differences were regarded significant if *P* < 0.05 (*). Higher levels of significance are indicated as ** (<0.01), *** (<0.001), or **** (<0.0001).

RESULTS

Whole cell voltage-clamp recordings were obtained from nRt neurons in mouse slices of six different age groups (p3/4, p5/6, p7/8, p9/11, p12/15, and p16/30); each group represents a total number of 50–57 neurons.

Identification of tGDPs in nRt

Examples of tGDPs at p4 and p8 are shown in Fig. 1A, 1–2, and B, 1–2, respectively. Here, we recorded tGDPs at -60 mV in voltage-clamp mode at room temperature in the presence APV (100 μM) and DNQX (20 μM) to block ionotropic glutamate receptors. We established three absolute criteria for all age groups to reliably isolate tGDPs from simple sIPSCs. The three basic properties include amplitudes >100 pA (≤ 700 pA), durations of 0.4–3 s (defined as time of decay from peak to 10% of the peak amplitude; i.e., 90% width), and multi-component appearance consisting of a minimum of three transients. Additionally, there was usually "build-up" of synaptic responses during each tGDP, such that several small transients preceded the peak response. This activity pattern occurred spontaneously at frequencies of 0.02–0.06 Hz and was completely abolished by GABA_AR antagonist SR 95531 (10 μM; Fig. 5C), thus we termed these events thalamic giant GABAergic spontaneous depolarizing potentials (tGDPs). In the following analysis, when we use the term tGDP, we are referring to the events (synaptic currents) that would cause membrane depolarization if they were recorded in current clamp. We used voltage-clamp experiments in this study as it allowed us to accurately detect and characterize the individual components of each multiphasic synaptic response. In Fig. 1, representative continuous recordings and individual tGDP barrages are shown at two distinct time points during development (Fig. 1, A and B). There were fewer individual transients within each tGDP at p3/4 (mean number of transients per tGDP = 4.34 ± 0.23) compared with tGDPs at p7/8 (Fig. 1B2, 5.63 ± 0.05) or at later time points (p9/11: 7.04 ± 0.07 ; P12/15: 4.93 ± 0.14 , not shown). In general, there were fewer and smaller transients during the decay phase (mean ratio between pre- and postpeak transients at p3/4 = 1:3.4; at p7/8 = 1:4.8 and at p12/15 = 1:3.9; ns as in the preceding text). tGDPs generally showed similar kinetic properties (e.g., amplitude, duration, time to peak) throughout the duration of a recording.

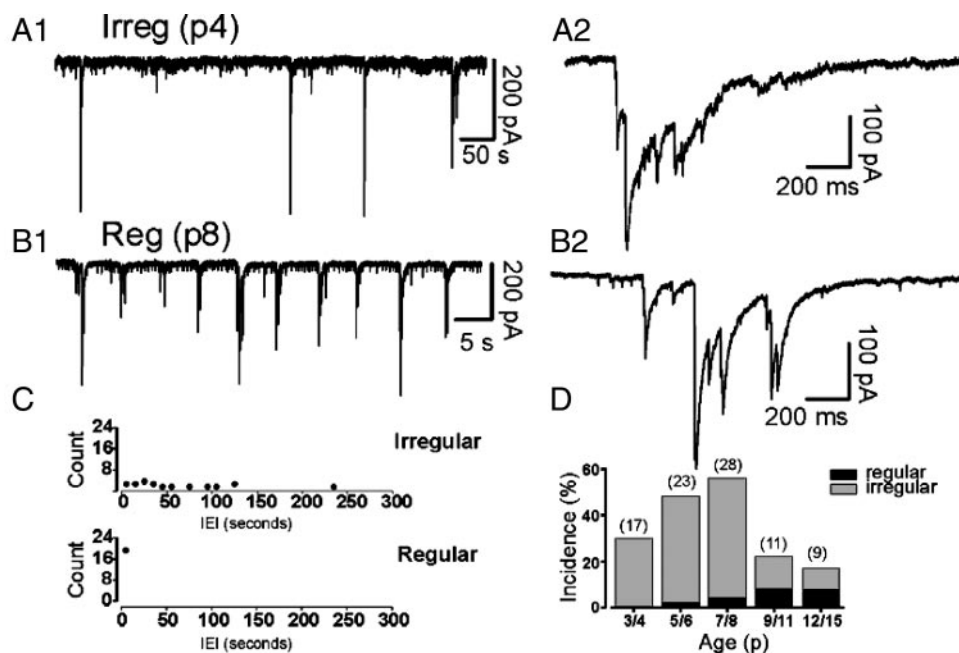


FIG. 1. Whole cell patch-clamp recordings of thalamic giant GABAergic spontaneous depolarizing potentials (tGDPs) in thalamic reticular nucleus (nRt) neurons. Sample traces illustrate prominent features of tGDPs recorded at p4–8. *A1*: example nRt cell at p4 shows predominately slow and large events with durations of ~ 800 ms and amplitudes ~ 400 pA. *A2*: representative tGDP from *A1* is shown on faster time scale. *B1*: recordings from a p8 cell. *B2*: representative tGDP from *B1* is shown on an extended time base. The recording in *A1* shows an *irregular* pattern with highly variable interevent intervals (IEIs) between tGDPs. In *B1*, a *regular* pattern with constant IEIs is displayed. *C*: histograms of tGDP IEIs for cells in *A* and *B* are shown where the p4 cell with irregular events (*top*) displays a random distribution, while the p8 cell with regular events has a narrow distribution (*bottom*). *D*: population data depict the incidence (%) of slices showing regular or irregular tGDP patterns as a function of age. tGDP incidence peaks at p7/8 and is mainly characterized by irregular pattern up until this point. Incidence decreases until p15 with a progressive increase in the proportion of slices with regularly patterned events. Numbers above each column indicate the number of slices at each developmental stage that displayed tGDPs.

tGDP regularity increases during development

The pattern of tGDP occurrence within individual slices was initially irregular at p3–4 and increased in regularity over the next several days of development (Fig. 1). Irregular patterns (e.g., Fig. 1, *A1* and *C, top*) were characterized by a high coefficient of variation of IEIs, whereas regular patterns (e.g., Fig. 1, *B1* and *C, bottom*) displayed events with a characteristic rhythmicity (see METHODS). The differences between these patterns can be seen in the IEI histograms in Fig. 1*C*. IEIs were distributed across a broad range (5–200 s) in the p4 slice in Fig. 1*A1*, whereas they were confined to values very near 5 s in the p8 slice in Fig. 1*B1*.

Figure 1*D* summarizes the incidence of tGDPs as percent of the total number of slices per age group with gray and black subdivisions representing the percentage of slices with regular and irregular patterns, respectively. At p3/4, tGDPs appeared in about a third of all slices ($n = 17$ of 54; 31%, Fig. 1*D*) and were characteristically irregular in their intervals. tGDP incidence increased significantly at p5/6 [$n = 23$ of 50 slices; 46% with only 1 of these slices (4%) showing a regular pattern], whereas peak activity was detected at p7/8, characterized by highest tGDP incidence [$n = 28$ of 50 slices; 56%; 2 slices (7%) with regular pattern] and frequency (lowest IEI, Table 1) of events. tGDP incidence declined in more mature slices at p9/11 and p12/15 ($n = 11$ of 50; 22%, and $n = 9$ of 50; 18%, respectively), whereas tGDPs were not observed later than p15. Regular tGDP patterns were observed with highest incidence at p9–p15 (37 and 55% of slices with tGDPs at these ages, respectively). Within slices where tGDPs were recorded, the briefest IEIs were observed at p7/8 (Table 1), and longer intervals were observed with slices from either more or less mature mice.

Developmental changes in tGDP properties

We identified tGDPs in 18–55% of all recordings depending on the age group. From this large sample, we randomly selected 9–20 cells per developmental stage for further analysis. Figure 2 presents a summary of population data illustrating the developmental changes in tGDPs from p3 to p15. At p3/4, tGDPs were characterized by peak current amplitudes between 108 and 666 pA. As shown in Fig. 2*A*, tGDP amplitudes at this age were significantly larger (mean amplitude = 399 ± 12 pA; $n = 15$; Fig. 2*A*) compared with all other age groups. Mean peak amplitude decreased over the following several days (mean amplitude at p5/6 = 219 ± 18 pA; $n = 20$, and at p12/15 = 108 ± 7 ; $n = 9$; $P < 0.00001$; 1-way ANOVA). We next analyzed the distribution of amplitudes for each age group (Fig. 2*B*). Amplitudes were calculated from a minimum of five cells per age group (n of events per cell > 15), and the histogram was fitted with a single Gaussian distribution. This figure illustrates that although amplitudes were overlapping in their distributions, their peak currents shifted to significantly smaller events in nRt neurons older than p5/6. The

TABLE 1. Interevent intervals during development

| Age | IEI, s |
|--------|-----------------|
| P3/4 | 51.7 ± 6.5 |
| P5/6 | 48.6 ± 8.1 |
| P7/8 | 37.3 ± 7.1 |
| P9/11 | 53.3 ± 9.2 |
| P12/15 | 57.6 ± 11.3 |

IEI, interevent interval.

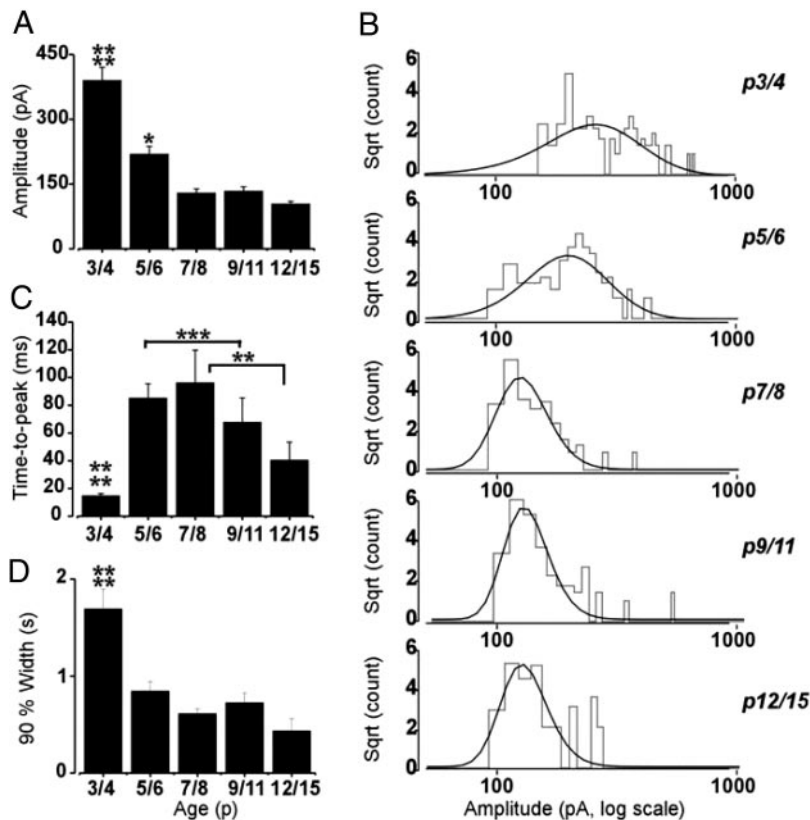


FIG. 2. Developmental changes of tGDP properties. *A*: tGDPs recorded at p3/4 displayed the largest peak currents and became progressively smaller with advancing age. *B*: histograms depicting tGDP amplitude distributions for each developmental stage show a significant leftward shift from p3/4 to p5/6 and p7/8 followed by stabilization at p7/8 levels. Amplitudes were calculated from a minimum of 5 cells per age group (>15 events per cell), and the histograms were fitted with single Gaussian distributions. *C*: although the time to peak (TTP) of tGDPs was highly variable at all ages studied (range between 1.2 and 71.4 ms; mean = 14.05 ± 1.76 ms), we observed a significant increase in the TTP between p3/4 and p7/8 ($P < 0.001$; 1-way ANOVA), followed by a marked decrease from p7/8 to p12/15 ($P < 0.0001$; 1-way ANOVA). *D*: tGDP duration (measured as 90% width) significantly decreased after p3/4 ($P < 0.0001$; 1-way ANOVA). *n* of cells at p3/4 = 15, p5/6 = 20, p7/8 = 20, p9/11 = 9, and at p12/15 = 9.

developmental decrease in tGDP amplitude was paralleled by a progressive reduction in duration (mean 90% width at p3/4 = 1692 ± 204 ms; $n = 15$, p7/8 = 613 ± 50 ms; $n = 20$ and at p12/15 = 535 ± 125 ms; $n = 9$, $P < 0.00001$; 1-way ANOVA, Fig. 2*D*). Change in TTP showed the opposite trend (Fig. 2*C*). At p3/4, values were significantly smaller (range between 1.2 and 71.4 ms, mean = 14.05 ± 1.76 ms; $n = 15$), compared with p7/8 (range between 1.9 and 115.5 ms, mean = 96.3 ± 23.4 ms; $n = 20$, $P < 0.001$; 1-way ANOVA). After p9/11, both the number of prepeak transients (p9/11 = 2.4 ± 0.3 ; $n = 11$, p12/15 = 1.64 ± 0.19 ; $n = 9$) and the TTP declined. In summary, we observed not only the highest incidence of tGDPs at p7/8 but also the highest frequency (shortest IELs, Table 1) and the longest TTP.

tGDPs do not arise from simple summation of sIPSCs

Multiphasic IPSCs could arise from concerted network events or from the nearly simultaneous occurrence of multiple individual spontaneous synaptic currents. To distinguish between these two possibilities, we calculated the total synaptic charge transferred per each 2-s period throughout a recording. Occasional summation of randomly occurring sIPSCs would be reflected by a continuous distribution of charge transferred per unit period. On the other hand, if tGDPs are generated by a mechanism distinct from sIPSCs, then we would expect to see a biphasic distribution with little charge transferred during periods with only sIPSCs and much greater charge transferred during tGDPs. Figure 3 shows example traces with tGDPs for slices from different age groups. In Fig. 3*A1*, a representative trace at p5 is displayed, whereas the charge transfer per 2-s window is shown in Fig. 3*A2*. Charge transfer was generally

quite low (<15 pC). Occasionally large sIPSCs were seen (Fig. 3*A*, 1 and 2*) with charge transfer on the order of 10 pC. However, tGDPs were associated with much greater charge (>50 pC). Thus charge transfer in this cell displayed a biphasic distribution (Fig. 3*A4*), inconsistent with the idea that tGDPs could arise from simple summation of sIPSCs. The distribution demonstrates a first peak (<30 pC), which represents sIPSC occurrence, and the second peak (>30 and <180 pC), representing tGDPs. An example at p9 is shown in Fig. 3*B*, which demonstrated the same biphasic distribution of charge transfer per unit time (Fig. 3*B*, 2 and 4), although there was a developmental decrease in overall charge transfer, consistent with the kinetic changes depicted in Fig. 2.

tGDPs are mediated by depolarizing GABA responses

Early in postnatal life, GABAergic transmission can be depolarizing and thus excitatory instead of inhibitory (Ben Ari et al. 1989; Cherubini et al. 1991). Depolarizing GABA responses contribute to giant depolarizing potentials (GDPs) in developing hippocampal circuits. They are generated by a synergism between excitatory GABAergic and ionotropic glutamatergic receptors (Ben-Ari et al. 1997; Cherubini et al. 1991; Owens et al. 1996). In immature hippocampal neurons, the reversal potential for chloride (E_{Cl^-}) is more depolarized than the resting membrane potential due to accumulation of intracellular chloride [Cl^-]_i (Cherubini et al. 1991). Therefore we tested whether the [Cl^-]_i concentration was higher in immature than in adult nRt neurons (Fig. 4). We used a noninvasive technique to estimate E_{GABA} by recording in cell-attached mode with high K^+ -filled pipettes (Verheugen et al. 1999). V_m was estimated based on the expected reversal

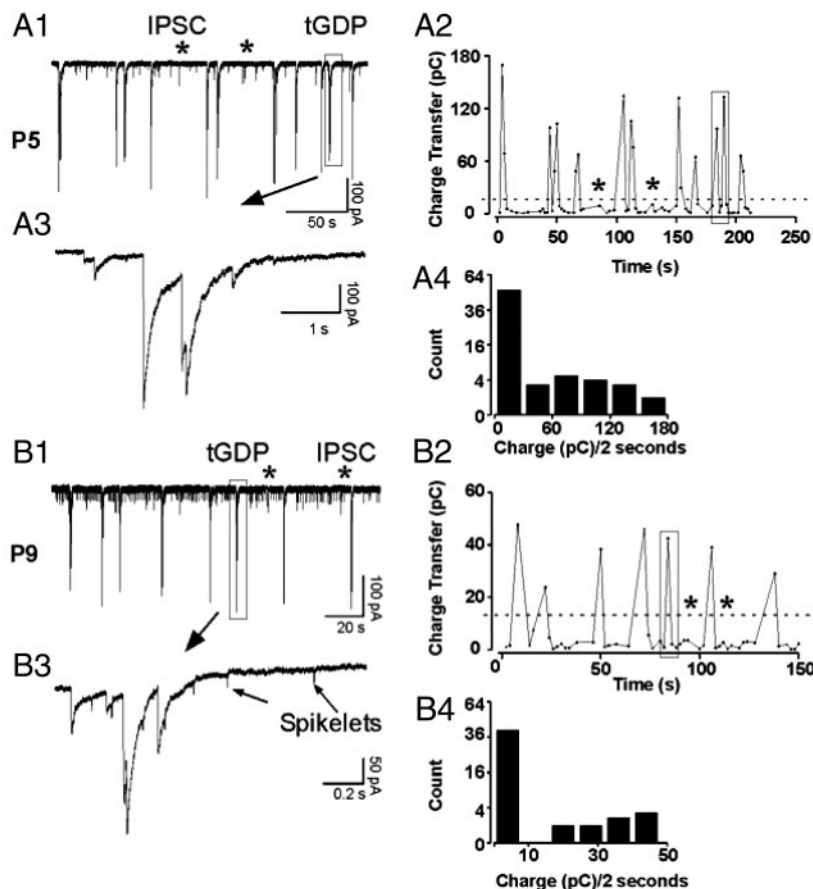


FIG. 3. Charge transfer differentiates between tGDPs and spontaneous inhibitory postsynaptic currents (sIPSCs) in nRt neurons. *A1*: sample trace depicting both sIPSCs (*) and tGDPs in a p5 nRt cell. The framed tGDP is shown on extended time scale in *A3*. *A2*: charge transfer (per 2-s bin) over the time course of the recording in *A1* depicts prominent differences in charge of tGDPs vs. sIPSCs. --- (at 15 pC), periods with or without tGDPs. The histogram in *A4* clearly shows 2 types of events, with most of the 2-s periods containing <30 pC charge (*, i.e., with sIPSCs only), and a smaller number with much larger charge transfer (up to >150 pC). *B*: tGDP vs. sIPSC charge in a p9 nRt cell, depicted as in *A*. Note the smaller charge transfer in the neuron at p9 compared with p5. Brief inward events in *B1* and *B3* are spikelets (presumed action potentials electrotonically propagated from presynaptic cells).

potential (~ 0 mV) for voltage-gated K^+ currents. Thus with isotonic K^+ in the pipette, K^+ currents reverse direction when V_m equals V_h . To determine whether E_{GABA} was hyperpolarized or depolarized compared with resting membrane potential in p14–20 nRt neurons, we measured the change in membrane potential produced by GABA application. Depolarizing voltage ramps (from $V_h = -100$ to $+200$ mV) were applied to elicit K^+ currents before (Fig. 4*A1*, top), during (A2, middle), and after (A3, bottom) bath application of $50 \mu\text{M}$ GABA. Figure 4*A1–3* shows averaged current responses ($n = 10$) to voltage ramps at p3. In control conditions, ramp stimuli activated voltage-gated K^+ currents, which were inward from onset up to ~ 55 mV and reversed direction at higher V_h values. For our calculations, we corrected for the linear leak current at values below activation threshold and then determined the E_K as the voltage at which the activated K^+ current response intersected the linear leak (“correction”). At p3, we calculated mean V_m in control as -77 ± 1 mV ($n = 3$). In the presence of $50 \mu\text{M}$ GABA, we observed a shift to more depolarized values for V_m , (mean V_m for p3 in presence of GABA: -65 ± 2 mV; $n = 3$). This effect was reversible during washout (mean V_m after washout: -83 ± 5 mV, $P < 0.01$, $n = 3$, 1-way ANOVA). By contrast, GABA induced a hyperpolarization in more mature neurons (p20, mean V_m in control: -87 ± 2 mV, in GABA: -96 ± 3 mV and during washout: -82 ± 4 mV, $P < 0.05$, $n = 4$, 1-way ANOVA). Figure 4*B* compares how the average V_m changed during GABA application for two representative neurons at p3 and p20. For recordings at p3 (Fig. 4*C*) GABA depolarized nRt V_m , and a similar, but not signif-

icant trend was seen at p7. By contrast, at p14–20, GABA hyperpolarized V_m . This is in accordance with findings that at more mature ages GABA acts mainly as “stabilizer” of V_m (Verheugen et al. 1999). In summary (Fig. 4*D*), we observed a significant depolarization of V_m in the presence of GABA at p3, compared with a smaller but significant hyperpolarization at p14–20. Presumably, active chloride extrusion mechanisms which maintain a lower $[\text{Cl}^-]_i$ concentration in adult neurons (Misgeld et al. 1986) are not yet fully developed at this age (Fukuda et al. 1998; Ganguly et al. 2001; Toyoda et al. 2003).

Potential contributions of ionotropic glutamate receptors to tGDPs

In the experiments described so far, we had applied APV+DNQX to isolate GABA_A R-mediated events. The presence of tGDPs under these conditions indicates that the activation of ionotropic glutamate receptors is not required for tGDP generation. To determine whether AMPA or NMDA receptors might nevertheless contribute to tGDP generation, we tested the effect of ionotropic glutamate receptor blockade on tGDPs in a separate series of experiments in p5–9 mice. The effects of bath-applied APV+DNQX are shown in Fig. 5, *A* and *B*, where we observed only minor changes, including a modest but significant reduction in tGDP amplitude (257 ± 34 to 170 ± 29 pA, $n = 8$; $P < 0.05$, paired Student’s *t*-test) without obvious changes in IEI or 90% width (not shown). Thus we conclude that ionotropic glutamate receptor activation is not essential for tGDP generation, indicating significant differences in the mechanism underlying the genera-

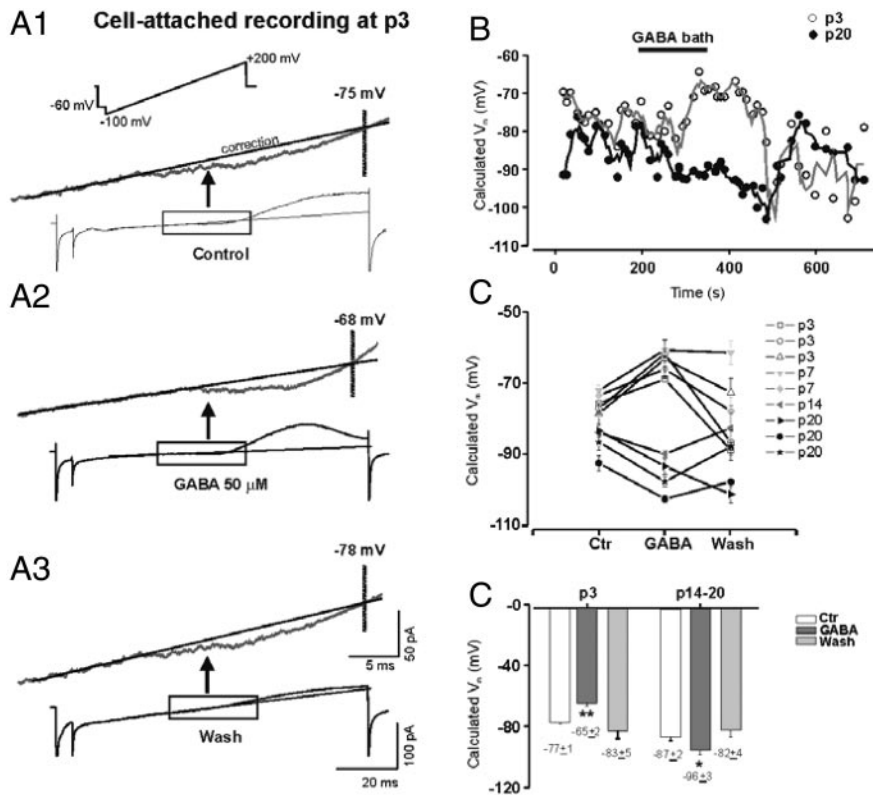


FIG. 4. Calculation of E_{GABA} in nRt neurons at different developmental stages. Cell-attached recordings (pipette solution contains 155 mM K^+) of voltage-gated K^+ currents in control condition and presence of GABA. Depolarizing voltage ramps were applied to activate K^+ currents (from $V_h = -100$ to $+200$ mV) to establish the K^+ reversal potential. In A, A1 shows V_m (-76 mV) in control condition in a p3 nRt cell. A2: GABA $_A$ R activation causes depolarization of the V_m to -69 mV in the same neuron. A3: depolarization is reversible during washout. B: GABA $_A$ R activation reversibly depolarizes V_m in a p3 neuron (\circ) but produces hyperpolarization in a p20 cell (\bullet). C: summary data show that GABA reversibly induces depolarization in all p3 and p7 cells, while hyperpolarizing p14–20 cells. D: population data for changes in V_m produced by bath application of GABA. Depolarization from -77 ± 1 to -65 ± 2 mV resulted at p3 ($P < 0.01$, $n = 3$) and hyperpolarization (-87.2 ± 2 to 96 ± 3 mV) at p14–20 ($P < 0.05$, $n = 4$, paired t -test).

tion of giant potentials in nRt compared with the CA3 region in hippocampus (Ben Ari et al. 1989). Finally, the GABA $_A$ R antagonist SR95531 (gabazine, GBZ) effectively blocked tGDP activity at all ages (Fig. 5C). This result provides further support that GABAergic transmission plays the central role in tGDP generation.

tGDPs are mediated by $\alpha 5$ subunit containing GABA $_A$ Rs

In mature neurons of the thalamic reticular nucleus, $\alpha 3$ subunits of the GABA $_A$ R are highly expressed, whereas other

alpha subunits are almost undetectable (Pirker et al. 2000; Wisden et al. 1992). We recently observed (Pangratz-Fuehrer et al. 2004) that the $\alpha 5$ subunit is transiently expressed in synaptic GABA $_A$ Rs in nRt during early development. Given that GABA $_A$ Rs in nRt do not express the $\alpha 1$ or $\alpha 2$ subunit, the final series of experiments was designed to determine whether tGDP properties are mediated by GABA $_A$ Rs containing $\alpha 3$ or $\alpha 5$. To distinguish between these two possibilities, we compared the effects of clonazepam (CZP, 100 nM) on tGDPs recorded from thalamic slices obtained from $\alpha 3$ (H126R) and their wild-type controls (WT; Fig. 6). The $\alpha 3$ (H126R) point-mutation (Low et al. 2000) affects selectively the GABA $_A$ R $\alpha 3$ subunit by rendering it insensitive to benzodiazepines (BZs) with otherwise normal function. We speculated that if tGDPs were mediated by $\alpha 3$ subunit-containing GABA $_A$ Rs, we would observe no BZ-induced effect in the mutant. Alternatively, if they were mediated by GABA $_A$ Rs containing $\alpha 5$, tGDPs would be enhanced. As shown in Fig. 6A, bath perfusion with CZP increased tGDP amplitude and decay kinetics to a similar extent in both genotypes. Example tGDPs in Fig. 6B and population data in Fig. 6C demonstrate that CZP strongly increased 90% width from 902 ± 70 to $1,319 \pm 95$ ms (46%) in WT and from 962 ± 106 to $1,544 \pm 146$ ms (60%) in $\alpha 3$ mutant mice ($n = 3$ for each genotype; $P < 0.01$, paired Student's t -test). Furthermore, tGDP amplitude was significantly increased by $\sim 25\%$ in both genotypes, in the WT from 198 ± 22 to 244 ± 28 pA and in the $\alpha 3$ mutant from 173 ± 22 to 213 ± 14 pA. The increase in decay time was not correlated with any alterations in IEs (not shown). In conclusion, because we did not observe any differences in the extent of CZP sensitivity between genotypes, the most likely explanation is that the $\alpha 5$ subunit primarily contributes to tGDP modulation by BZs during the first postnatal week.

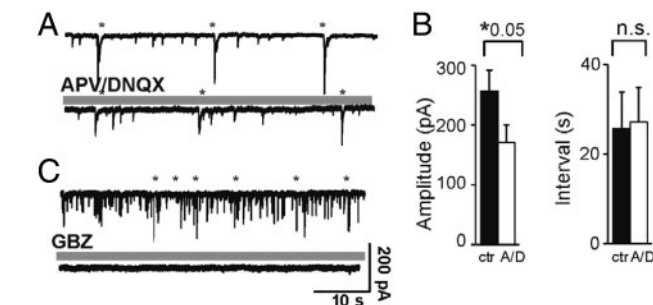


FIG. 5. tGDPs are GABAergic and can occur in the absence of glutamate receptor activation. A: tGDPs persist during ionotropic glutamate receptor blockade. Top: control artificial cerebrospinal fluid (ACSF); *, tGDPs. Bottom: obtained in same cell after 10 min of (\pm)-2-amino-5-phosphonopentanoic acid (APV)/6,7-dinitro-quinoxaline-2,3-dione (DNQX) application. tGDPs persist but at reduced amplitude, in the presence of APV/DNQX (A/D). B: population data for effects of APV/DNQX (A/D, 100 and 20 μ M, respectively) on tGDP amplitude and IEI. On average, tGDP amplitude (left) was reduced by 34% ($P < 0.05$; $n = 8$; 57%) by A/D without concurrent changes in IEI (right). C: tGDPs are dependent on GABA $_A$ receptor activation. Top: control ACSF. Bottom: after 6 min of bath application of the GABA $_A$ receptor antagonist gabazine (GBZ, 10 μ M) Scale bars in C apply for A.

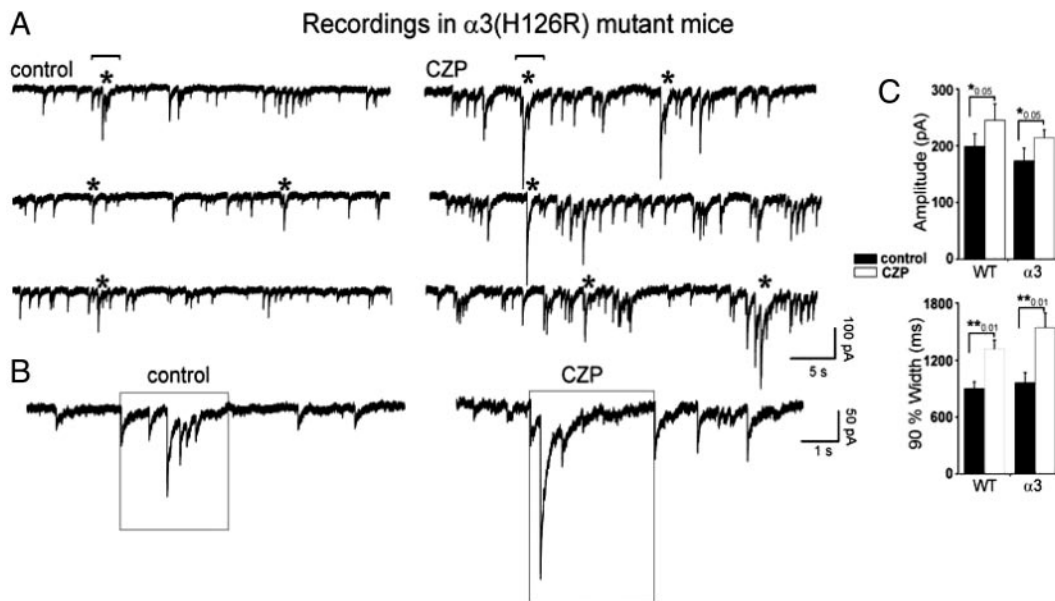


FIG. 6. tGDPs are mediated by $\alpha 5$ -containing GABA_ARs and are Benzodiazepine sensitive. *A*: recording from a neuron obtained from p5 $\alpha 3$ (H126R) mutant mouse, in control condition (*left*), and in the presence of clonazepam (CZP, 100 nM, *right*). *B*: representative tGDPs in control and CZP are shown on extended time scale to illustrate increase of both amplitude and decay time. *C*: population data demonstrating CZP-dependent increases in amplitude ($P < 0.05$) and duration (90% width, $P < 0.01$) for WT and $\alpha 3$ (H126R), respectively ($n = 3$ per phenotype; paired Student's *t*-test).

DISCUSSION

In the present study, voltage-clamp recordings in immature thalamic mouse slices have clearly shown the existence of patterned spontaneous synaptic activity in the nRt. In particular, we have observed GABA-mediated tGDPs within the first 2 wk of postnatal life. This suggests that in thalamus, similar to other developing networks, spontaneous intrinsic activity within nRt may regulate development and refinement of neuronal circuits. Further work will be required to determine the specific role tGDPs play in the maturation of nRt circuitry.

Developmental profile of tGDPs in nRt

tGDPs share similar properties with neonatal patterns observed in other maturing networks. However, our data indicate that tGDP activity is unique in some ways among endogenous network activities. Although the time window for incidence of spontaneous network activity was similar in all published studies (in the 1st week of postnatal life), the incidence of tGDPs in thalamic slices was considerably lower than that of giant depolarizing potentials (GDPs) (Ben Ari et al. 1989) or early neonatal oscillations (ENOs) (Garaschuk et al. 1998) in hippocampus CA3 and CA1 slices, respectively. tGDPs were present in only 31–56% of all thalamic slices between p3 and p8, whereas GDPs and ENOs were observed in ~85% of hippocampal recordings between p0/1 and p8 (Ben Ari et al. 1989; Garaschuk et al. 1998). It is noteworthy that our studies were carried out in mice in contrast to studies in hippocampus that recorded from slices obtained from rats. In addition, we cannot exclude that tGDPs are already present in nRt neurons younger than p3/4.

Patterned activity in nRt

With the discovery of spontaneous activity in immature networks (Ben Ari et al. 1989; Garaschuk et al. 1998; Wong et al. 1993; Yuste et al. 1992), several different neuronal patterns

have been described so far, such as synchronous and asynchronous patterns in the CA1 region of rat hippocampus (Garaschuk et al. 1998). Furthermore, previous studies have correlated early network activity with the appearance of Ca^{2+} oscillations (Ben Ari et al. 1989; Flint et al. 1999; Garaschuk et al. 1998; Wong et al. 1993; Yuste et al. 2005). Although patterns of GDPs and ENOs are generally rhythmic, giant GABAergic events in nRt display a developmentally regulated time course that gradually transforms early “irregular” activity at p3/4 into “regular” activity in neurons $> p8$.

Potential mechanisms underlying tGDPs

The exact mechanisms for generation of immature network activities are incompletely understood. In hippocampus (Ben Ari et al. 1989; Garaschuk et al. 1998) and the retina (Wong et al. 1993), a key role has been attributed to the excitatory influence of the neurotransmitter GABA. For example, the generation of GDPs in hippocampus is based on joint operation of glutamate and GABA_A receptors. However, in nRt, blocking ionotropic glutamate receptors merely reduced tGDP amplitude, whereas blocking GABA_ARs abolished them completely. The fact that the reversal potential of GABA (E_{GABA}) for immature nRt neurons at p5 is depolarized compared with adult cells suggests that GABA is functionally excitatory and tGDPs are primarily GABA mediated. The reticular nucleus is characterized by strong interconnections between individual GABAergic cells that are mediated by both chemical and electrical synapses (Deleuze and Huguenard 2006). The depolarizing influence of the former in early development (Fig. 4) together with the excitatory coupling afforded by gap junctions would create a recurrent excitatory network within nRt. This would explain the persistence of the tGDPs even in the absence of ionotropic glutamatergic excitation. On the other hand, the fact that tGDPs are detectable even after p8 indicates that GABA-mediated depolarization of nRt neurons might not be

the only mechanism that can trigger tGDP generation. We therefore suggest that other mechanisms could contribute to a transient increase in intracellular calcium, such as metabotropic glutamate receptor (mGluR) activation. Studies in juvenile rats have shown that the activation of mGluRs in nRt can coordinate synchronous rhythms among electrically coupled neurons (Long et al. 2004).

Furthermore, the reciprocal recurrent connectivity between relay and nRt neurons may create an accessory network that could amplify the internal network response. Hence, the mildly suppressive effects of CNQX and APV on tGDPs (Fig. 5) may result from disruption of the accessory network.

Taken together, these data suggest that several mechanisms may be responsible for generating and propagating patterned activity in the immature nRt, including spontaneous GABA release, perhaps triggered by voltage-gated Ca^{2+} channels; glutamate release from thalamocortical or corticothalamic axon terminals with resulting activation of mGluRs; astroglia associated Ca^{2+} oscillations as observed for the thalamic ventrobasal complex (Crunelli et al. 2002; Parri and Crunelli 2002; Parri et al. 2001); and/or via gap-junction-mediated synchronization.

Are tGDPs mediated by a different GABA_AR subtype?

In the mammalian brain, GABA_ARs mediate the majority of GABAergic signaling and provide fast inhibition. GABA_ARs are constructed as pentameric ion channels with several binding sites for allosteric modulators, such as BZs. The kinetic properties and allocation of these receptors is determined by the subunit assembly, particularly by the α subunit isoform (Sieghart and Sperk 2002). Although considerable research had been devoted to unraveling biophysical properties of these individual GABA_AR subtypes (Barnard et al. 1998; Mody and Pearce 2004; Okada et al. 2000; Ortinski et al. 2004; Sieghart and Sperk 2002; Vicini et al. 1986), less attention has been paid to whether a distinct α subtype is associated with GABA_AR-mediated spontaneous activity in immature networks. We have observed that the expression of GABA_ARs containing $\alpha 5$ subunits precedes GABA_ARs containing the $\alpha 3$ subunit in mouse nRt neurons during very early development (Pangratz-Fuehrer et al. 2004). When we compared the time course of tGDP incidence with the expression of the GABA_AR $\alpha 5$ subunit in nRt, we found that both peaked at the end of the first postnatal week. These results are further supported by recent findings of high GABA_AR $\alpha 5$ subunit expression in nRt at p5, whereas only low expression was detected at p0 and p10 (Studer et al. 2006). Essentially no expression of $\alpha 1$ (Pangratz-Fuehrer et al. 2004) or $\alpha 2$ (Studer et al. 2006) subunits could be detected at the end of the first postnatal week. Taken together with our results that clonazepam strongly enhanced tGDPs in immature nRt neurons of the BZ-insensitive $\alpha 3$ mutant, we suggest that tGDPs are primarily mediated by the GABA_AR $\alpha 5$ subtype. $\alpha 3$ and $\alpha 5$ GABA_AR subtypes may be co-expressed for a short period of time prior to synapse maturation around p9. Further support for a transient co-expression of $\alpha 3$ and $\alpha 5$ is suggested by the heightened GABA potency in p5/9 rat nRt neurons compared with p18/25, and p58/74 rats (Gibbs et al. 1996). The turnover and re-arrangement of GABA_AR subtypes is responsible for mature inhibitory signal transduction in a variety of systems (Dunning et al. 1999; Hollrigel and Soltesz 1997; Okada et al. 2000; Tia et al.

1996; Vicini et al. 2001). Disruptions of the normal developmental sequence may produce long-lasting changes in network excitability. Thus a mouse mutant lacking the adult GABA_AR subtype ($\alpha 1$), which is normally highly expressed in mature neocortical neurons, showed impaired γ oscillations. This may have resulted from a failure of the synaptic receptors to attain a mature phenotype (fast kinetics) required to support high-frequency oscillations (Bosman et al. 2005). By analogy, disruptions in the development of nRt circuitry may then prevent normal development of the spindle generating circuitry potentially leading to disorders of sleep and AE.

Conclusion

In summary, we report the existence of spontaneous, large-amplitude depolarizing synaptic events (tGDPs) in developing nRt neurons. These events differ in terms of generation and propagation from neonatal spontaneous activity previously described for other brain regions. The tGDPs are mainly mediated by the GABA_AR $\alpha 5$ -subtype and reflect a time and location specific network pattern in nRt. The spontaneous tGDPs are intrinsic (generated within nRt), and we speculate that they play a role in the development of intra-thalamic connectivity and furthermore that the switch to $\alpha 3$ -containing GABA_ARs is associated with functional maturation of the circuit. Because well-regulated inhibitory output from nRt is central to normal rhythm generation in the thalamocortical system, perturbation of tGDPs might alter activity-dependent nRt network development and disrupt formation of the normal rhythm generating circuitry.

ACKNOWLEDGMENTS

We thank T. Anderson, C. Deleuze, and S. Brown for useful comments on this manuscript.

GRANTS

This work was supported by National Institute of Neurological Disorders and Stroke Grants NS-06477 and NS-34774 and by the Austrian Science Fund (FWF) Project J2222-B04.

REFERENCES

- Barnard EA, Skolnick P, Olsen RW, Mohler H, Sieghart W, Biggio G, Braestrup C, Bateson AN, Langer SZ. International Union of Pharmacology. XV. Subtypes of gamma-aminobutyric acid-A receptors: classification on the basis of subunit structure and receptor function. *Pharmacol Rev* 50: 291–313, 1998.
- Ben Ari Y, Cherubini E, Corradetti R, Gaiarsa JL. Giant synaptic potentials in immature rat CA3 hippocampal neurons. *J Physiol* 416: 303–325, 1989.
- Ben Ari Y, Khazipov R, Leinekugel X, Caillard O, Gaiarsa JL. GABA_A, NMDA and AMPA receptors: a developmentally regulated 'menage a trois'. *Trends Neurosci* 20: 523–529, 1997.
- Ben Ari Y, Rovira C, Gaiarsa JL, Corradetti R, Robain O, Cherubini E. GABAergic mechanisms in the CA3 hippocampal region during early postnatal life. *Prog Brain Res* 83: 313–321, 1990.
- Bosman LW, Heinen K, Spijker S, Brussaard AB. Mice lacking the major adult GABA_A receptor subtype have normal number of synapses, but retain juvenile IPSC kinetics until adulthood. *J Neurophysiol* 94: 338–346, 2005.
- Cherubini E, Gaiarsa JL, Ben Ari Y. GABA: an excitatory transmitter in early postnatal life. *Trends Neurosci* 14: 515–519, 1991.
- Crunelli V, Blethyn KL, Cope DW, Hughes SW, Parri HR, Turner JP, Toth TI, Williams SR. Novel neuronal and astrocytic mechanisms in thalamocortical loop dynamics. *Philos Trans R Soc Lond B Biol Sci* 357: 1675–1693, 2002.
- Deleuze C, Huguenard JR. Distinct electrical and chemical connectivity maps in the thalamic reticular nucleus: potential roles in synchronization and sensation. *J Neurosci* 26: 8633–8645, 2006.
- Destexhe A, Contreras D, Sejnowski TJ, Steriade M. A model of spindle rhythmicity in the isolated thalamic reticular nucleus. *J Neurophysiol* 72: 803–818, 1994.

- Dunning DD, Hoover CL, Soltesz I, Smith MA, O'Dowd DK.** GABA(A) receptor-mediated miniature postsynaptic currents and alpha-subunit expression in developing cortical neurons. *J Neurophysiol* 82: 3286–3297, 1999.
- Feller MB.** Spontaneous correlated activity in developing neural circuits. *Neuron* 22: 653–656, 1999.
- Flint AC, Dammerman RS, Kriegstein AR.** Endogenous activation of metabotropic glutamate receptors in neocortical development causes neuronal calcium oscillations. *Proc Natl Acad Sci USA* 96: 12144–12149, 1999.
- Fukuda A, Tanaka M, Yamada Y, Muramatsu K, Shimano Y, Nishino H.** Simultaneous optical imaging of intracellular Cl^- in neurons in different layers of rat neocortical slices: advantages and limitations. *Neurosci Res* 32: 363–371, 1998.
- Ganguly K, Schinder AF, Wong ST, Poo M.** GABA itself promotes the developmental switch of neuronal GABAergic responses from excitation to inhibition. *Cell* 105: 521–532, 2001.
- Garaschuk O, Hanse E, Konnerth A.** Developmental profile and synaptic origin of early network oscillations in the CA1 region of rat neonatal hippocampus. *J Physiol* 507: 219–236, 1998.
- Gibbs JW III, Schroder GB, Coulter DA.** GABA_A receptor function in developing rat thalamic reticular neurons: whole cell recordings of GABA-mediated currents and modulation by clonazepam. *J Neurophysiol* 76: 2568–2579, 1996.
- Gonzalez-Islas C, Wenner P.** Spontaneous network activity in the embryonic spinal cord regulates AMPAergic and GABAergic synaptic strength. *Neuron* 49: 563–575, 2006.
- Goodman CS, Shatz CJ.** Developmental mechanisms that generate precise patterns of neuronal connectivity. *Cell* 72 Suppl: 77–98, 1993.
- Gummer AW, Mark RF.** Patterned neural activity in brain stem auditory areas of a prehearing mammal, the tammar wallaby (*Macropus eugenii*). *Neuroreport* 5: 685–688, 1994.
- Hollrigel GS, Soltesz I.** Slow kinetics of miniature IPSCs during early postnatal development in granule cells of the dentate gyrus. *J Neurosci* 17: 5119–5128, 1997.
- Huguenard JR, Prince DA.** Intrathalamic rhythmicity studied in vitro: nominal T-current modulation causes robust antioscillatory effects. *J Neurosci* 14: 5485–5502, 1994.
- Huntsman MM, Porcello DM, Homanics GE, DeLorey TM, Huguenard JR.** Reciprocal inhibitory connections and network synchrony in the mammalian thalamus. *Science* 283: 541–543, 1999.
- Jouvet-Mounier D, Astic L, Lacote D.** Ontogenesis of the states of sleep in rat, cat, and guinea pig during the first postnatal month. *Dev Psychobiol* 2: 216–239, 1970.
- Kandler K, Katz LC.** Coordination of neuronal activity in developing visual cortex by gap junction-mediated biochemical communication. *J Neurosci* 18: 1419–1427, 1998.
- Katz LC, Callaway EM.** Development of local circuits in mammalian visual cortex. *Annu Rev Neurosci* 15: 31–56, 1992.
- Katz LC, Shatz CJ.** Synaptic activity and the construction of cortical circuits. *Science* 274: 1133–1138, 1996.
- Lenard HG.** The development of sleep spindles during the first 2 years of life. *Electroencephalogr Clin Neurophysiol* 29: 217, 1970.
- Long MA, Landisman CE, Connors BW.** Small clusters of electrically coupled neurons generate synchronous rhythms in the thalamic reticular nucleus. *J Neurosci* 24: 341–349, 2004.
- Low K, Crestani F, Keist R, Benke D, Brunig I, Benson JA, Fritschy JM, Rulicke T, Bluethmann H, Mohler H, Rudolph U.** Molecular and neuronal substrate for the selective attenuation of anxiety. *Science* 290: 131–134, 2000.
- McCormick DA, Trent F, Ramoa AS.** Postnatal development of synchronized network oscillations in the ferret dorsal lateral geniculate and perigeniculate nuclei. *J Neurosci* 15: 5739–5752, 1995.
- Meister M, Wong RO, Baylor DA, Shatz CJ.** Synchronous bursts of action potentials in ganglion cells of the developing mammalian retina. *Science* 252: 939–943, 1991.
- Metcalf D.** The ontogenesis of sleep-awake states from birth to 3 months. *Electroencephalogr Clin Neurophysiol* 28: 421, 1970.
- Misgeld U, Deisz RA, Dodt HU, Lux HD.** The role of chloride transport in postsynaptic inhibition of hippocampal neurons. *Science* 232: 1413–1415, 1986.
- Mody I, Pearce RA.** Diversity of inhibitory neurotransmission through GABA(A) receptors. *Trends Neurosci* 27: 569–575, 2004.
- Okada M, Onodera K, Van Renterghem C, Sieghart W, Takahashi T.** Functional correlation of GABA(A) receptor alpha subunits expression with the properties of IPSCs in the developing thalamus. *J Neurosci* 20: 2202–2208, 2000.
- Ortinski PI, Lu C, Takagaki K, Fu Z, Vicini S.** Expression of distinct α subunits of GABA_A receptor regulates inhibitory synaptic strength. *J Neurophysiol* 92: 1718–1727, 2004.
- Owens DF, Boyce LH, Davis MB, Kriegstein AR.** Excitatory GABA responses in embryonic and neonatal cortical slices demonstrated by gramicidin perforated-patch recording and calcium imaging. *J Neurosci* 16: 6414–6423, 1996.
- Pangratz-Fuehrer S, Huguenard JR.** Postnatal GABA(A) receptor turnover in the thalamic reticular nucleus in mice. *Soc Neurosci Abstr* 31: 160–168, 2004.
- Parri HR, Crunelli V.** Astrocytes, spontaneity, and the developing thalamus. *J Physiol* 96: 221–230, 2002.
- Parri HR, Gould TM, Crunelli V.** Spontaneous astrocytic Ca^{2+} oscillations in situ drive NMDAR-mediated neuronal excitation. *Nat Neurosci* 4: 803–812, 2001.
- Pirker S, Schwarzer C, Wieselthaler A, Sieghart W, Sperk G.** GABA(A) receptors: immunocytochemical distribution of 13 subunits in the adult rat brain. *Neuroscience* 101: 815–850, 2000.
- Sieghart W, Sperk G.** Subunit composition, distribution and function of GABA(A) receptor subtypes. *Curr Top Med Chem* 2: 795–816, 2002.
- Sohal VS, Huntsman MM, Huguenard JR.** Reciprocal inhibitory connections regulate the spatiotemporal properties of intrathalamic oscillations. *J Neurosci* 20: 1735–1745, 2000.
- Spitzer NC.** Activity-dependent neuronal differentiation prior to synapse formation: the functions of calcium transients. *J Physiol* 96: 73–80, 2002.
- Steriade M, Deschenes M, Domich L, Mulle C.** Abolition of spindle oscillations in thalamic neurons disconnected from nucleus reticularis thalami. *J Neurophysiol* 54: 1473–1497, 1985.
- Steriade M, Domich L, Oakson G, Deschenes M.** The deafferented reticular thalamic nucleus generates spindle rhythmicity. *J Neurophysiol* 57: 260–273, 1987.
- Steriade M, Llinas RR.** The functional states of the thalamus and the associated neuronal interplay. *Physiol Rev* 68: 649–742, 1988.
- Studer R, von Boehmer L, Haenggi T, Schweizer C, Benke D, Rudolph U, Fritschy JM.** Alteration of GABAergic synapses and gephyrin clusters in the thalamic reticular nucleus of GABA_A receptor alpha3 subunit-null mice. *Eur J Neurosci* 24: 1307–1315, 2006.
- Tia S, Wang JF, Kotchabhakdi N, Vicini S.** Developmental changes of inhibitory synaptic currents in cerebellar granule neurons: role of GABA(A) receptor alpha 6 subunit. *J Neurosci* 16: 3630–3640, 1996.
- Toyoda H, Ohno K, Yamada J, Ikeda M, Okabe A, Sato K, Hashimoto K, Fukuda A.** Induction of NMDA and GABA_A receptor-mediated Ca^{2+} oscillations with KCC2 mRNA downregulation in injured facial motoneurons. *J Neurophysiol* 89: 1353–1362, 2003.
- Verheugen JA, Fricker D, Miles R.** Noninvasive measurements of the membrane potential and GABAergic action in hippocampal interneurons. *J Neurosci* 19: 2546–2555, 1999.
- Vicini S, Alho H, Costa E, Mienville JM, Santi MR, Vaccarino FM.** Modulation of gamma-aminobutyric acid-mediated inhibitory synaptic currents in dissociated cortical cell cultures. *Proc Natl Acad Sci USA* 83: 9269–9273, 1986.
- Vicini S, Ferguson C, Prybylowski K, Kralic J, Morrow AL, Homanics GE.** GABA(A) receptor alpha subunit deletion prevents developmental changes of inhibitory synaptic currents in cerebellar neurons. *J Neurosci* 21: 3009–3016, 2001.
- von Krosigk M, Bal T, McCormick DA.** Cellular mechanisms of a synchronized oscillation in the thalamus. *Science* 261: 361–364, 1993.
- Warren RA, Agmon A, Jones EG.** Oscillatory synaptic interactions between ventroposterior and reticular neurons in mouse thalamus in vitro. *J Neurophysiol* 72: 1993–2003, 1994.
- Warren RA, Jones EG.** Maturation of neuronal form and function in a mouse thalamo-cortical circuit. *J Neurosci* 17: 277–295, 1997.
- Wisden W, Laurie DJ, Monyer H, Seeburg PH.** The distribution of 13 GABA_A receptor subunit mRNAs in the rat brain. I. Telencephalon, diencephalon, mesencephalon. *J Neurosci* 12: 1040–1062, 1992.
- Wong RO.** Retinal waves and visual system development. *Annu Rev Neurosci* 22: 29–47, 1999.
- Wong RO, Meister M, Shatz CJ.** Transient period of correlated bursting activity during development of the mammalian retina. *Neuron* 11: 923–938, 1993.
- Yuste R, MacLean JN, Smith J, Lansner A.** The cortex as a central pattern generator. *Nat Rev Neurosci* 6: 477–483, 2005.
- Yuste R, Peinado A, Katz LC.** Neuronal domains in developing neocortex. *Science* 257: 665–669, 1992.